Inorg. Chem. **2005**, *44*, 5872–5881

Dinitrosyl Iron Complexes (DNICs) $[L_2Fe(NO)_2]^-$ (L = Thiolate): Interconversion among $\{Fe(NO)_2\}^9$ DNICs, $\{Fe(NO)_2\}^{10}$ DNICs, and [2Fe-2S] Clusters, and the Critical Role of the Thiolate Ligands in Regulating NO Release of DNICs

Fu-Te Tsai, Show-Jen Chiou, Ming-Che Tsai, Ming-Li Tsai, Hsiao-Wen Huang, Ming-Hsi Chiang, and Wen-Feng Liaw*

Department of Chemistry, National Tsing Hua University, Hsinchu 30013, Taiwan

Received April 5, 2005

Dinitrosyl iron complex $[(-SC_7H_4SN)_2Fe(NO)_2]^-$ (**1**) was prepared by reaction of $[S_5Fe(NO)_2]^-$ and bis(2-benzothiozolyl) disulfide. In synthesis of the analogous dinitrosyl iron compounds (DNICs), the stronger electron-donating thiolates $[RS]^-$ (R = C_6H_4-*o*-$NHCOCH_3$, C_4H_3S, $C_6H_4NH_2$, Ph), compared to $[-SC_7H_4SN]^-$ of complex **1**, trigger thiolate-ligand substitution to yield $[(-SC_6H_4$-*o*-$NHCOCH_3)_2Fe(NO)_2]^-$ (**2**), $[(-SC_4H_3S)_2Fe(NO)_2]^-$ (**3**), and $[(SPh)_2Fe(NO)_2]^-$ (**4**), respectively. At 298 K, complexes **2** and **3** exhibit a well-resolved five-line EPR signal at $g = 2.038$ and 2.027, respectively, the characteristic g value of DNICs. The magnetic susceptibility fit indicates that the resonance hybrid of $\{Fe^+(^\bullet NO)_2\}^9$ and $\{Fe^-(^+NO)_2\}^9$ in **2** is dynamic by temperature. The IR ν_{NO} stretching frequencies (ranging from (1766, 1716) to (1737, 1693) cm^{-1} (THF)) of complexes **1**–**4** signal the entire window of possible electronic configurations for such stable and isolable $\{Fe(NO)_2\}^9$ $[(RS)_2Fe(NO)_2]^-$. The NO-releasing ability of $\{Fe(NO)_2\}^9$ $[(RS)_2Fe(NO)_2]^-$ is finely tuned by the coordinated thiolate ligands. The less electron-donating thiolate ligands coordinated to $\{Fe(NO)_2\}^9$ motif act as better NO-donor DNICs in the presence of NO-trapping agent $[Fe(S,S$-$C_6H_4)_2]_2^{2-}$. Interconversion between $\{Fe(NO)_2\}^9$ $[(RS)_2Fe(NO)_2]^-$ and $\{Fe(NO)_2\}^{10}$ $[(Ph_3P)_2Fe(NO)_2]$ was verified in the reaction of (a) $[(RS)_2Fe(NO)_2]^-$, 10 equiv of PPh_3 and sodium-biphenyl, and (b) 2 equiv of thiol, $[RS]^-$, and $[(Ph_3P)_2Fe(NO)_2]$, respectively. The biomimetic reaction cycle, transformation between $\{Fe(NO)_2\}^9$ $[(RS)_2Fe(NO)_2]^-$ and $\{Fe(NO)_2\}^9$ $[(R'S)_2Fe(NO)_2]^-$, reversible interconversion of $\{Fe(NO)_2\}^9$ and $\{Fe(NO)_2\}^{10}$ DNICs, and degradation/reassembly of [2Fe–2S] clusters may decipher and predict the biological cycle of interconversion of $\{Fe(NO)_2\}^9$ DNICs, $\{Fe(NO)_2\}^{10}$ DNICs, and the [Fe–S] clusters in proteins.

Introduction

In vivo, nitric oxide can be stabilized and stored in the form of dinitrosyl iron complexes with proteins (protein-bound DNICs) and is probably released from cells in the form of low-molecular-weight dinitrosyl iron complexes (low-molecular-weight DNICs (LMW-DNICs)).[1,2] Dinitrosyl iron complexes (DNICs) and *S*-nitrosothiols (RSNO) have been known to be two possible forms for storage and transport of NO in biological systems.[3] DNICs are intrinsic NO-derived species that can appear in various NO over-producing tissues.[4] Depending on the micro-environment, LMW-DNICs can provide at least two types of nitrosylating modification of proteins, forming either protein-*S*-nitroso-thiols or protein-bound DNICs.[4] Also, DNICs have been suggested as intermediates of iron-catalyzed degradation and formation of *S*-nitrosothiols.[5,6] LMW-DNICs may release NO to various targets.[7] As observed in cells or tissues, LMW-

* To whom correspondence should be addressed. E-mail: wfliaw@mx.nthu.edu.tw.

(1) (a) Foster, M. W.; Cowan, J. A. *J. Am. Chem. Soc.* **1999**, *121*, 4093. (b) Reginato, N.; McCrory, C. T. C.; Pervitsky, D.; Li, L. *J. Am. Chem. Soc.* **1999**, *121*, 10217.
(2) Cooper, C. E. *Biochim. Biophys. Acta* **1999**, *1411*, 290.
(3) (a) Ford, P. C.; Lorkovic, I. M. *Chem. Rev.* **2002**, *102*, 993. (b) Hayton, T. W.; Legzdins, P.; Sharp, W. B. *Chem. Rev.* **2002**, *102*, 935. (c) Butler, A. R.; Megson, I. L. *Chem. Rev.* **2002,** *102*, 1155−1166. (d) Ford, P. C.; Bourassa, J.; Miranda, K.; Lee, B.; Lorkovic, I.; Boggs, S.; Kudo, S.; Laverman, L. *Coord. Chem. Rev.* **1998**, *171*, 185.
(4) (a) Boese, M.; Mordvintcev, P. I.; Vanin, A. F.; Busse, R.; Mulsch, A. *J. Biol. Chem.* **1995**, *270*, 29224−29229. (b) Mulsch, A.; Mordvintcev, P. I.; Vanin, A. F.; Busse, R. *FEBS Lett* **1991**, *294*, 252−256. (c) Henry, Y.; Lepoivre, M.; Drapier, J. C.; Ducrocq, C.; Boucher, J. L.; Guissani, A. *FASEB J.* **1993**, *7*, 1124−1134.

10.1021/ic0505044 CCC: $30.25
Published on Web 07/01/2005

DNICs exerting cyclic GMP-independent effects were attributed to nitrosylating modification of proteins via the transfer of NO or $Fe(NO)_2$ unit yielding protein *S*-nitrosothiols or protein-bound DNICs.[8] Transfer of $Fe(NO)_2$ motif of LMW-DNICs resulting in the formation of protein-bound DNICs serving as a NO-storage site was also demonstrated in isolated arteries, although the persistent *S*-nitrosylation of protein is another mechanism of formation of releasable NO-storage site in arteries.[4] In particular, a recent report showed that both DNICs-CYS (CYS = cysteine) and DNICs-GSH (GSH = glutathione) elicited a NO release associated relaxant effect in isolated arteries, and a faster rate of NO release from DNICs-CYS than from DNICs-GSH was observed.[9] Also, it has been proposed that free thiols/thiolates can displace the proteins of the protein-bound DNICs via thiolate exchange to afford LMW-DNICs.[4,10]

As LMW-DNICs react readily with protein thiols to give nitrosothiols, LMW-DNICs can exist only at very low levels in tissue. In contrast, proteinaceous DNICs are stable for hours in the absence of low-molecular-weight thiols and can accumulate in high concentrations in tissues.[2,10] Also, it has been shown that LMW-DNICs with cysteine (DNICs-CYS) or glutathione (DNICs-GSH) serving as the coordination ligand are much more unstable than the protein-bound DNICs existing with cysteine residues of proteins as ligands.[11]

Free NO produced from NO synthase was shown to bind to iron-sulfide groups of intracytoplasmic proteins or to thiolate groups of proteins in the presence of free iron.[1,2] Recently, Ding and co-workers showed that the ferredoxin [2Fe−2S] clusters and [4Fe−4S] cluster of the *E. coli* endonuclease III can be modified by nitric oxide to form protein-bound DNICs. In the repair of nitric oxide modified ferredoxin [2Fe−2S] and [4Fe−4S] clusters, cysteine desulfurase (IscS) and L-cysteine are required to regenerate the iron−sulfur clusters in vitro.[12]

We have shown that reversible transformation of the $\{Fe^+(^\bullet NO)_2\}^9$ complex $[S_5Fe(NO)_2]^-$ to the $[S_5Fe(\mu\text{-}S)_2FeS_5]^{2-}$ cluster by photolysis in the presence of the NO-acceptor reagent $[(C_4H_8O)Fe(S,S\text{-}C_6H_4)_2]^-$, characterized by UV−vis, EPR, and XAS, is consistent with reports of in vitro repair of nitric oxide modified [2Fe−2S] ferredoxin by cysteine desulfurase and L-cysteine.[13] Reversibly, the [2Fe−2S] cluster $[S_5Fe(\mu\text{-}S)_2FeS_5]^{2-}$ treated with nitric oxide in THF is transformed into the dinitrosyl iron complex $[S_5Fe(NO)_2]^-$.[13a] Isolation and characterization of the diamagnetic diiron $[(ON)Fe(S,S\text{-}C_6H_4)_2Fe(NO)_2]^-$ complex containing a $\{Fe(NO)_2\}^9$ dinitrosyl iron motif may be useful for taking into consideration the existence (formation) of the metalloprotein-bound DNICs in the anaerobic reaction between iron−sulfur protein and nitric oxide. Noticeably, complex $[(ON)Fe(S,S\text{-}C_6H_4)_2Fe(NO)_2]^-$ with no characteristic isotopic EPR signal of $g = 2.03$ represents a new member of a class of dinitrosyl iron complexes.[14]

The function and role of coordinated thiolate ligands of the $\{Fe(NO)_2\}^9$ LMW-DNICs $[(RS)_2Fe(NO)_2]^-$,[15] the difference(s) and functional role of $\{Fe(NO)_2\}^9$ and $\{Fe(NO)_2\}^{10}$ LMW-DNICs, the route(s) leading to the formation of LMW-DNICs, the conditions for convertibility and interconversion mechanism among $\{Fe(NO)_2\}^9$ LMW-DNICs, $\{Fe(NO)_2\}^{10}$ LMW-DNICs, and [Fe−S] clusters are the principal questions to be raised in the chemistry of dinitrosyl iron complexes. In these structural and reaction model studies, the influences of the coordinated thiolate ligands of $\{Fe(NO)_2\}^9$ DNICs $[(RS)_2Fe(NO)_2]^-$ (RS = thiolates) on the ability of NO release in the presence of NO-trapping reagent $[Fe(S,S\text{-}C_6H_4)_2]_2^{2-}$, transformation between $\{Fe(NO)_2\}^9$ $[(RS)_2Fe(NO)_2]^-$ and $\{Fe(NO)_2\}^9$ $[(R'S)_2Fe(NO)_2]^-$ and interconversion among $\{Fe(NO)_2\}^9$ DNICs, $\{Fe(NO)_2\}^{10}$ DNICs, and [2Fe−2S] clusters were demonstrated. In addition, the resonance-hybrid electronic structures of $\{Fe^+(^\bullet NO)_2\}^9$ and $\{Fe^-(^+NO)_2\}^9$ in DNICs **2** are suggested based on the magnetic susceptibility fit.

Results and Discussion

Synthesis of the dark red $[PPN][(-SC_7H_4SN)_2Fe(NO)_2]$ (**1**) by reaction of $[PPN][S_5Fe(NO)_2]$ and bis(2-benzothiozolyl)disulfide in 1:1 stoichiometry was investigated in THF under a N_2 atmosphere at ambient temperature (Scheme 1a).[13a] In contrast, complex $[S_5Fe(NO)_2]^-$ does not initiate RS−SR (R = *o*-$C_6H_4NHCOCH_3$, C_4H_3S, and Ph) activation to yield dinitrosyl iron thiolate complexes $[(RS)_2Fe(NO)_2]^-$. Complex **1** is soluble in THF/CH_3CN and is moderately air-sensitive in solution but is stable to air for weeks in the solid state. Complex **1** exhibits two IR ν_{NO} bands (1766 s, 1716 s cm^{-1} (THF)). The shifts of ν_{NO} to higher wavenumbers in complex **1** as compared to complex $[(PhS)_2Fe(NO)_2]^-$ (1737 s, 1693 s cm^{-1} (THF)) are consistent with the less electron-donating character of $[-SC_7H_4SN]^-$ as compared to that of

(5) (a) Vanin, A. F. *Biochem.* (Moscow) **1998**, *63*, 782. (b) Vanin, A. F.; Malenkova, I. V.; Serezhenkov, V. A. *Nitric Oxide Biol. Chem.* **1997**, *1*, 191. (c) Vanin, A. F.; Stukan, R. A.; Manukhina, E. B. *Biochim. Biophys. Acta* **1996**, *1295*, 5.
(6) (a) Hayton, T. W.; Legzdins, P.; Sharp, W. B. *Chem. Rev.* **2002**, *102*, 935. (b) Wang, P. G.; Xian, M.; Tang, X.; Wu, X.; Wen, Z.; Cai, T.; Janczuk, A. J. *Chem. Rev.* **2002** *102*, 1091.
(7) Ueno, T.; Susuki, Y.; Fujii, S.; Vanin, A. F.; Yoshimura, T. *Biochem. Pharmacol.* **2002**, *63*, 485−493.
(8) Wiegant, F. A.; Malyshev, I. Y.; Kleschyov, A. L.; van Faassen, E.; Vanin, A. F. *FEBS Lett.* **1999**, *455*, 179−182.
(9) Alencar, J. L.; Chalupsky, K.; Sarr, M.; Schini-Kerth, V.; Vanin, A. F.; Stoclet, J.-C.; Muller, B. *Biochem. Pharmacol.* **2003**, *66*, 2365−2374.
(10) (a) Radi, R.; Beckman, J. S.; Bush, K. M.; Freeman, B. A. *J. Biol. Chem.* **1991**, *266*, 4244−4250. (b) Mulsch, A. *Drug Res.* **1994**, *44*, 3a, 408−411. (c) Vanin, A. F.; Mordvintcev, P. I.; Hauschildt, S.; Mulsch, A. *Biochim. Biophys. Acta* **1993**, *1177*, 37−42.
(11) (a) Boese, M.; Keese, M. A.; Becker, K.; Busse, R.; Mulsch, A. *J. Biol. Chem.* **1997**, *272*, 21767−21773. (b) Keese, M. A.; Boese, M.; Mulsch, A.; Schirmer, R. H.; Becker, K. *Biochem. Pharmacol.* **1997**, *54*, 1307−1313.
(12) (a) Rogers, P. A.; Ding, H. *J. Biol. Chem.* **2001**, *276*, 30980−30986. (b) Yang, W.; Rogers, P. A.; Ding, H. *J. Biol. Chem.* **2002**, *277*, 12868−12873. (c) Rogers, P. A.; Eide, L.; Klungland, A.; Ding, H. *DNA Repair* **2003**, *2*, 809−817.
(13) (a) Tsai, M.-L.; Chen, C.-C.; Hsu, I.-J.; Ke, S.-C.; Hsieh, C.-H.; Chiang, K.-A.; Lee, G.-H.; Wang, Y.; Liaw, W.-F. *Inorg. Chem.* **2004**, *43*, 5159−5167. (b) Lee, C.-M.; Hsieh, C.-H.; Dutta, A.; Lee, G.-H.; Liaw, W.-F. *J. Am. Chem. Soc.* **2003**, *125*, 11492−11493. (c) Liaw, W.-F.; Chiang, C.-Y.; Lee, G.-H.; Peng, S.-M.; Lai, C.-H.; Darensbourg, M. Y. *Inorg. Chem.* **2000**, *39*, 480−484.
(14) Chen, H.-W.; Lin, C.-W.; Chen, C.-C.; Yang, L.-B.; Chiang, M.-H.; Liaw, W.-F. *Inorg. Chem.* **2005**, *44*, 3226−3232.
(15) Enemark, J. H.; Feltham, R. D. *Coord. Chem. Rev.* **1974**, *13*, 339.

Scheme 1

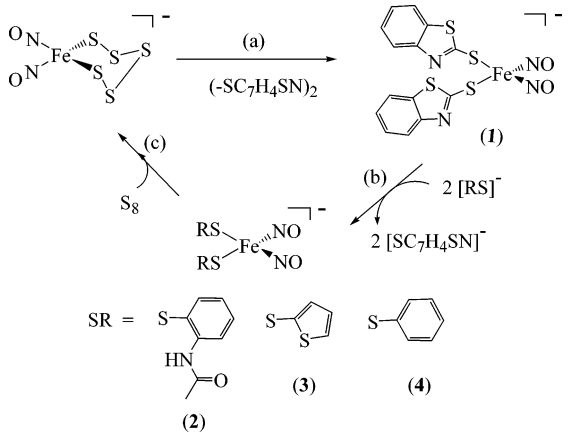

Scheme 2

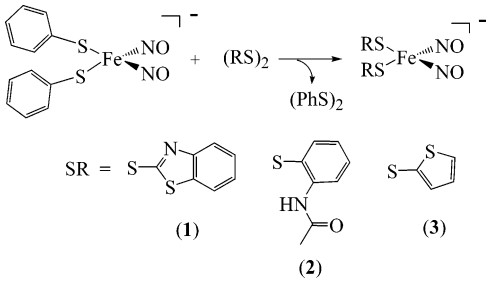

the $[SPh]^-$.[16] Complex **1** has two bands in the electronic absorption spectrum at 799, 465 nm (THF).

The coordinated $[-SC_7H_4SN]^-$ ligands of complex **1** could be replaced by the stronger electron-donating thiolates, $[SC_6H_4$-*o*-$NHC(O)CH_3]^-$, $[-SC_4H_3S]^-$, and $[SPh]^-$. As shown in Scheme 1b, reaction of complex **1** and 2 equiv of $[SC_6H_4$-*o*-$NHC(O)CH_3]^-$, $[-SC_4H_3S]^-$, and $[SPh]^-$, respectively, in CH_3CN solution at room temperature rapidly yielded the stable complexes $[PPN][(SC_6H_4$-*o*-$NHC(O)CH_3)_2Fe(NO)_2]$ (**2**), $[PPN][(-SC_4H_3S)_2Fe(NO)_2]$ (**3**), and $[PPN][(SPh)_2Fe(NO)_2]$ (**4**),[16b] characterized by IR, UV−vis, and single-crystal X-ray diffraction, and $[PPN][SC_7H_4SN]$ was identified by ^1H NMR. The $[Fe(NO)_2]$ unit remains intact while the thiolate ligands exchange. In a similar fashion, the ligand-displacement reaction was also displayed by complex **2** and 2 equiv of $[-SC_4H_3S]^-/[SPh]^-$, respectively. In contrast, reaction of complex **1** and 2 equiv of [PPN][SEt] in CH_3CN does not lead to the isolation of the stable $[(EtS)_2Fe(NO)_2]^-$. This result implicates that the $\{Fe(NO)_2\}^9$ center shows less affinity for the stronger electron-donating alkylthiolate ligands $[SR]^-$ to yield the stable/isolable $[(RS)_2Fe(NO)_2]^-$ DNICs. Clearly, binding of thiolate ligands to $\{Fe(NO)_2\}^9$ core displays high selectivity. The ligand-substitution reactions are expected to be driven by the formation of the $Fe-(SR)_2$ bonds that are sufficient to place $\{Fe(NO)_2\}^9$ DNICs **2**−**4** in an optimum electronic condition. Obviously, the electron-donating ability of thiolates (based on ν_{NO} stretching frequencies of DNICs) controlling binding of thiolates to $\{Fe(NO)_2\}^9$ core might be important to the existence of $\{Fe(NO)_2\}^9$ DNICs $[(RS)_2Fe(NO)_2]^-$. The IR spectra for all anionic DNICs **1**−**4** had the same pattern but differed slightly in positions. The shift of IR ν_{NO} frequency to the lower wavenumbers for the series of complexes **1**−**4** (1766 s, 1716 s (**1**); 1752 s, 1705 s (**2**); 1743 s, 1698 s (**3**); 1737 s, 1693 s (**4**) cm^{-1} (THF)) indicates a trend of increasing electronic donation of the $[SR]^-$ ligands to the $\{Fe(NO)_2\}$ motif, which also reflects on reduction potentials of complexes **1**−**4** (vide infra). Presumably, the ν_{NO} stretching frequencies of complexes **1**−**4** falling into the range from (1766, 1716) to (1737, 1693) cm^{-1} (THF) present the entire window of possible electronic configurations for the stable and isolable $\{Fe(NO)_2\}^9$ $[(RS)_2Fe(NO)_2]^-$.[16] That is, the electron-donating ability of ligands $[-SC_7H_4SN]^-$, $[SC_6H_4$-*o*-$NHC(O)CH_3]^-$, $[-SC_4H_3S]^-$, and $[SPh]^-$ are the few that form stable $\{Fe(NO)_2\}^9$ $[(RS)_2Fe(NO)_2]^-$.

In contrast to complex **1**, conversion of complexes **2**−**4** to $[S_5Fe(NO)_2]^-$ was displayed when THF solution of complexes **2**−**4** was reacted with S_8, respectively, at ambient temperature; the shift in ν_{NO} from 1752, 1705 (**2**) (1743, 1698 (**3**); 1737, 1693 (**4**) cm^{-1} (THF)) to 1739, 1695 cm^{-1} (THF) is in accord with the formation of $[S_5Fe(NO)_2]^-$ (Scheme 1c). These results show that $\{Fe(NO)_2\}^9$ DNICs $[(RS)_2Fe(NO)_2]^-$, $[(R'S)_2Fe(NO)_2]^-$, and $[S_5Fe(NO)_2]^-$ are chemically interconvertible (Scheme 1).

In complex **2**, the presence of intramolecular [N−H···S] interactions was verified in the solid state by the observation of an IR ν_{N-H} stretching band 3303 cm^{-1} (KBr)[17] and subsequently confirmed by a single-crystal X-ray diffraction study. In comparison with the infrared ν(NO) and ν(CO) spectra (1752 s, 1705 vs, 1690 vs cm^{-1} (THF)) of $[(NO)_2Fe(SC_6H_4$-*o*-$NHC(O)CH_3)_2]^-$, the absorption bands at 1718 s, 1673 vs, and 1690 vs cm^{-1} in THF solution of $[(^{15}NO)_2Fe(SC_6H_4$-*o*-$NHC(O)CH_3)_2]^-$ are unambiguously assigned to the $\nu(^{15}NO)$ and ν(CO) stretching frequencies, respectively. At 298 K, complexes **2** and **3** exhibit a well-resolved five-line EPR spectrum with signal at $g = 2.038, 2.027$, the characteristic g value of DNICs, and the hyperfine coupling constants of 2.27 and 2.38 G, respectively.

In contrast to complex **1**, which rapidly forms the dinitrosyl iron complexes **2**−**4** by the thiolate-ligand-exchange route described in Scheme 1, complex **4** does not react with $[-SC_7H_4SN]^-$, $[SC_6H_4$-*o*-$NHC(O)CH_3]^-$, and $[-SC_4H_3S]^-$ ligands via thiolate-ligand exchange to form complexes **1**−**3**, respectively. Dinitrosyl iron complexes **1**−**3** were, alternatively, prepared by reacting complex **4** with disulfides $(SR)_2$ (R = C_7H_4SN, C_6H_4-*o*-$NHCOCH_3$, and C_4H_3S), respectively, in THF in a 1:1 ratio (Scheme 2). Similarly, the ligand-displacement reaction was also displayed by reaction of complex **3** and $(2$-*S*-$C_7H_4SN)_2$. This result implicates that the stronger electron-donating, coordinated thiolates of

(16) (a) Chiang, C.-Y.; Miller, M. L.; Reibenspies, J. H.; Darensbourg, M. Y. *J. Am. Chem. Soc.* **2004**, *126*, 10867−10874. (b) Strasdeit, H.; Krebs, B.; Henkel, G. *Z. Naturforsch.* **1986**, *41b*, 1357−1362. (c) Baltusis, L. M.; Karlin, K. D.; Rabinowitz, H. N.; Dewan, J. C.; Lippard, S. J. *Inorg. Chem.* **1980**, *19*, 2627−2632.

(17) (a) Okamura, T.; Takmizawa, S.; Ueyama, N.; Nakamura, A. *Inorg. Chem.* **1998**, *37*, 18−28. (b) Ueyama, N.; Yamada, Y.; Okamura, T.; Kimura, S.; Nakamura, A. *Inorg. Chem.* **1996**, *35*, 6473−6484. (c) Ueyama, N.; Okamura, T.; Nakamura, A. *J. Am. Chem. Soc.* **1992**, *114*, 8129−8137. (d) Chiou, S. J.; Riordan, C. G.; Rheingold, A. L. *PNAS* **2003**, *100*, 3695−3700.

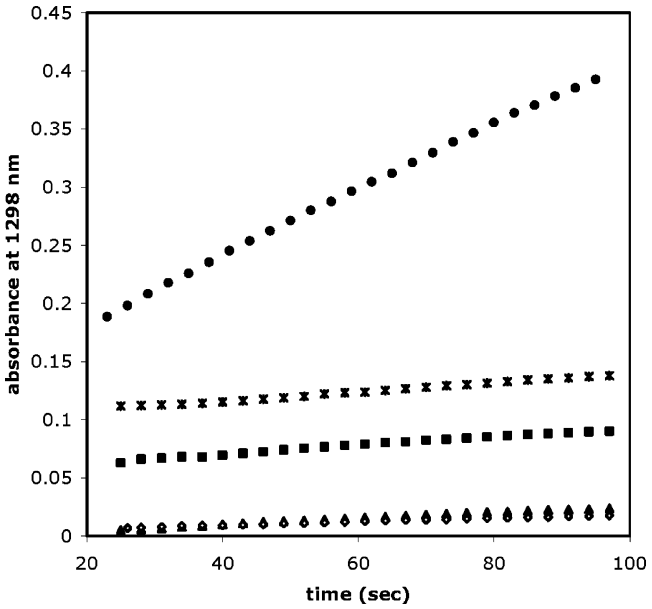

Figure 1. The plot of electronic absorbance vs time for the reactions of complexes **1** (●), **2** (∗), **3** (■), **4** (▲), and $[S_5Fe(NO)_2]^-$ (◊) with NO-trapping complex $[Fe(S,S\text{-}C_6H_4)_2]_2^{2-}$ in 1:1 stoichiometry. The study was monitored by the formation of product $[(NO)Fe(S,S\text{-}C_6H_4)_2]^-$ with an intense absorbance of 1298 nm in DMSO at 18 °C. The concentration of complexes **1**−**4** and $[S_5Fe(NO)_2]^-$ is 1.1×10^{-3} M.

$[(R'S)_2Fe(NO)_2]^-$ may trigger the S−S bond activation of $(RS)_2$ species to form the stable $[(RS)_2Fe(NO)_2]^-$.

On the basis of electronic structure of $\{Fe(NO)_2\}$ core of dinitrosyl iron complexes, the known stable LMW-DNICs can be classified into the paramagnetic $\{Fe(NO)_2\}^9$ DNICs coordinated by thiolate ligands and the diamagnetic $\{Fe(NO)_2\}^{10}$ DNICs coordinated by CO, PPh_3, and N-containing ligands.[13,16a,18] Upon reaction of complexes **1**−**4** and 2 equiv of NO-trapping agent $[(C_4H_8O)Fe(S,S\text{-}C_6H_4)_2]^-$ (or 1 equiv of $[Fe(S,S\text{-}C_6H_4)_2]_2^{2-}$) in THF, respectively, the iron-bound NO molecules of complexes **1**−**4** are released and bound to $[(C_4H_8O)Fe(S,S\text{-}C_6H_4)_2]^-$ to form $[(NO)Fe(S,S\text{-}C_6H_4)_2]^-$.[13b] In our previous report,[13a] we have demonstrated the reversible transformation between $[S_5Fe(NO)_2]^-$ and $[S_5Fe(\mu\text{-}S)_2FeS_5]^{2-}$. Reactions of $[S_5Fe(NO)_2]^-$ and NO trapping agent $[Fe(S,S\text{-}C_6H_4)_2]_2^{2-}$ in DMSO yielded $[(NO)Fe(S,S\text{-}C_6H_4)_2]^-$ and $[S_5Fe(\mu\text{-}S)_2FeS_5]^{2-}$ with $k_{obs} = 1.5\ (3) \times 10^{-2}\ s^{-1}$ (DMSO, 18 °C). For comparisons of NO-releasing activity of DNICs **1**−**4** and $[S_5Fe(NO)_2]^-$, the representative time courses of NO release trapped by 1 equiv of $[Fe(S,S\text{-}C_6H_4)_2]_2^{2-}$ in DMSO was monitored by the formation of $[(NO)Fe(S,SC_6H_4)_2]^-$ with an intense absorption band at 1298 nm, as shown in Figure 1. This result demonstrates that $\{Fe(NO)_2\}^9$ LMW-DNICs $[(RS)_2Fe(NO)_2]^-$ containing the less electron-donating, coordinated-thiolate ligands $[RS]^-$ display the better NO-donor activity; i.e., NO-donor ability: **1** > **2** > **3** > **4** > $[S_5Fe(NO)_2]^-$. Obviously, the distinct electron-donating strength of thiolate ligands bound to the $\{Fe(NO)_2\}^9$ motif may serve to modulate the NO-releasing ability of DNICs $[(RS)_2Fe(NO)_2]^-$. Such a regulatory role of thiolate/sulfide ligands in the $\{Fe(NO)_2\}^9$ DNICs $[(RS)_2Fe(NO)_2]^-/[S_5Fe(NO)_2]^-$ may be critical for $[(RS)_2Fe(NO)_2]^-$ to serve as a NO storage/NO transporter in biological systems.[9] These experimental results support the theory that the electronic structure of $[Fe(NO)_2]$ core of $\{Fe(NO)_2\}^9$ DNICs $[(SR)_2Fe(NO)_2]^-$ is best described as $\{Fe^+(^\bullet NO)_2\}$,[9] consistent with the observation in photolysis of $[S_5Fe(NO)_2]^-$.[13a] However, the magnetic susceptibility fit suggests that the electronic structure of $[Fe(NO)_2]$ core of DNICs $[(SR)_2Fe(NO)_2]^-$ is best described as a resonance hybrid of $\{Fe^-(^+NO)_2\}^9$ and $\{Fe^-(^{+\bullet}NO)_2\}$,[9] discussed in the following magnetic susceptibility study.

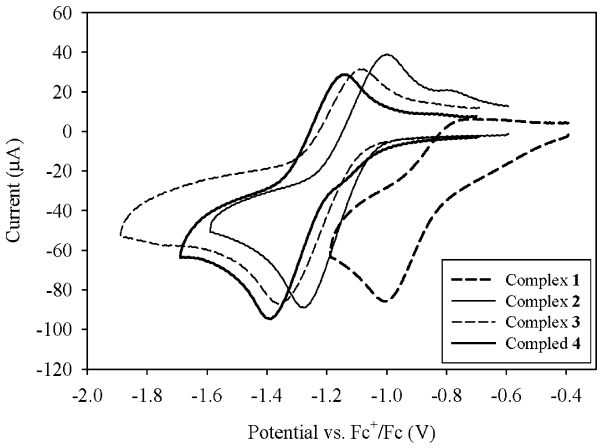

Figure 2. Cyclic voltammograms of a 1.25 mM CH_3CN solution of complexes **1** (bold dashed line), **2** (thin solid), **3** (thin dashed), and **4** (bold solid) in 0.05 M [TBA][PF_6] with a glassy carbon working electrode at a scan rate of 1 V s^{-1}.

The proposed electronic structure $\{Fe^+(^\bullet NO)_2\}^9$ of $[Fe(NO)_2]$ core of DNICs $[(SR)_2Fe(NO)_2]^-$ is also reflected in the NO ligand lability of complexes **1**−**4**. The reversibility of NO ligand lability of complexes **1**−**4** was demonstrated by exposing the THF solution of $[(RS)_2Fe(^{15}NO)_2]^-$ to a ^{14}-NO atmosphere. Complex $[(RS)_2Fe(^{15}NO)_2]^-$ (R = C_7H_4-SN, C_6H_4-*o*-$NHCOCH_3$, C_4H_3S, Ph) was stable under purge of ^{14}NO gas in THF at room temperature for 2 min. At the end of this time, the product was the completely enriched $[(SR)_2Fe(^{14}NO)_2]^-$. In the case of $\{Fe(NO)_2\}^{10}$ DNICs $[(Ph_3P)_2Fe(^{15}NO)(^{14}NO)]$, complex $[(Ph_3P)_2Fe(^{15}NO)(^{14}NO)]$ did not show the reversibility of NO ligand lability when a THF solution of $[(Ph_3P)_2Fe(^{15}NO)(^{14}NO)]$ was exposed to a ^{14}NO atmosphere. From the above evidence, it is further inferred that the anionic $\{Fe(NO)_2\}^9$ DNICs $[(SR)_2Fe(NO)_2]^-$ may act as a $^\bullet$NO-donor species.

Interconversion of $\{Fe(NO)_2\}^9$ and $\{Fe(NO)_2\}^{10}$ DNICs. Cyclic voltammograms of complexes **1**−**4** recorded in CH_3CN are shown in Figure 2. One electrochemical event, due to the $\{Fe(NO)_2\}^9$−$\{Fe(NO)_2\}^{10}$ couple,[13c] is centered at −0.93, −1.30, −1.31, and −1.33 V ($E_{1/2}$ vs Fc^+/Fc), respectively. Reduction of the $\{Fe(NO)_2\}^9$ DNICs at the least potential for $[(PhS)_2Fe(NO)_2]^-$ is in accord with the strongest ability of $[PhS]^-$ in the series of donating strength: $[PhS]^-$ > $[-SC_4H_3S]^-$ > $[SC_6H_4$-*o*-$NHC(O)CH_3]^-$ > $[-SC_7H_4$-$SN]^-$. Pseudo-reversibility (E_a-$E_c \geq 200$ mV) of the redox process at a scan rate of 1 V s^{-1} indicates that the

(18) (a) Reginato, N.; McCrory, C. T. C.; Pervitsky, D.; Li, L. *J. Am. Chem. Soc.* **1999**, *121*, 10217−10218. (b) Hedberg, L.; Hedberg, K.; Satija, S. K.; Swanson, B. I. *Inorg. Chem.* **1985**, *24*, 2766. (c) Albano, V. G.; Araneo, A.; Bellon, P. L.; Ciani, G.; Manassero, M. *J. Organomet. Chem.* **1974**, *67*, 413.

Scheme 3

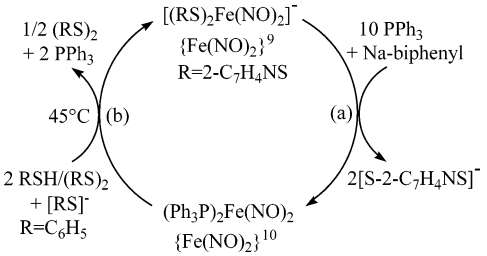

$\{Fe(NO)_2\}^{10}$ DNICs with thiolate coordination are not as stable as their $\{Fe(NO)_2\}^9$ counterpart. It implies that higher electron density about the Fe center in the $\{Fe(NO)_2\}^{10}$ DNICs is not in favor of an electron-rich coordination sphere by anionic thiolate ligation anymore. Reversible interconversion between the $\{Fe(NO)_2\}^9$ and $\{Fe(NO)_2\}^{10}$ DNICs probably occurs in the presence of less donating ligands other than thiolates. Neutral ligand such as triphenylphosphine is a better candidate in quest of stabilizing the $\{Fe(NO)_2\}^{10}$ DNICs. For the interconversion of $\{Fe(NO)_2\}^9$ $[(RS)_2Fe(NO)_2]^-$ and $\{Fe(NO)_2\}^{10}$ $[L_2Fe(NO)_2]$ (L = neutral ligands), complexes **1**−**4** cannot directly convert to $[(Ph_3P)_2Fe(NO)_2]$ upon addition of 2 equiv of PPh_3 to complexes **1**−**4** in THF at room temperature. Conversion of $\{Fe(NO)_2\}^9$ **1** to $[(Ph_3P)_2Fe(NO)_2]$ was observed when THF solution of complex **1** and 10 equiv of PPh_3 was mixed with sodium-biphenyl THF solution under N_2 at −40 °C. The reaction was monitored by FTIR immediately, and the ν_{NO} spectrum shows two strong absorption bands at 1682, 1639 cm^{-1} (THF) temporarily assigned as the formation of $\{Fe(NO)_2\}^{10}$ $[(2\text{-}S\text{-}C_7H_4NS)(Ph_3P)Fe(NO)_2]^-$ intermediate. The reaction solution was then stirred at room temperature overnight and yielded $\{Fe(NO)_2\}^{10}$ $[(Ph_3P)_2Fe(NO)_2]$. The transformation of complex **1** to $[(Ph_3P)_2Fe(NO)_2]$ under mild conditions may be accounted for by the following reaction sequences: the rapid electron transfer from sodium-biphenyl to $[(SR)_2Fe(NO)_2]^-$ leads to the buildup of $\{Fe(NO)_2\}^{10}$ $[(SR)(Ph_3P)Fe(NO)_2]^-$ intermediate. This reactive $\{Fe(NO)_2\}^{10}$ $[(SR)(Ph_3P)Fe(NO)_2]^-$ is then driven by the formation of $[(Ph_3P)_2Fe(NO)_2]$ via ligand-displacement (Scheme 3a). The role of sodium-biphenyl is interpreted as mediating the destabilization of $[(RS)_2Fe(NO)_2]^-$ by one-electron reduction.

In the transformation of $\{Fe(NO)_2\}^{10}$ $[(Ph_3P)_2Fe(NO)_2]$ to $\{Fe(NO)_2\}^9$ DNICs $[(RS)_2Fe(NO)_2]^-$, 2 equiv of thiols and 1 equiv of $[RS]^-$ are required to promote conversion of $\{Fe(NO)_2\}^{10}$ $[(Ph_3P)_2Fe(NO)_2]$ to $\{Fe(NO)_2\}^9$ $[(RS)_2Fe(NO)_2]^-$ (R = C_6H_5 (**4**), *p*-Cl−C_6H_4 (**5**), 2,4,5-Cl_3−C_6H_2 (**6**)) in CH_3CN at 45 °C (Scheme 3b). The following reaction sequences were proposed to explain the observed conversion: oxidative addition of RSH to $\{Fe(NO)_2\}^{10}$ $[(Ph_3P)_2Fe(NO)_2]$, followed by acid−base reaction of thiol with the proposed $[(RS)(H)Fe(NO)_2]$ leads to the buildup of $\{Fe(NO)_2\}^8$ $[(RS)_2Fe(NO)_2]$ intermediate. The subsequent reduction by $[RS]^-$ ligand yields $\{Fe(NO)_2\}^9$ DNICs $[(RS)_2Fe(NO)_2]^-$ and $^1/_2(RS)_2$. Alternatively, the conversion of $\{Fe(NO)_2\}^{10}$ $[(Ph_3P)_2Fe(NO)_2]$ to $\{Fe(NO)_2\}^9$ $[(RS)_2Fe(NO)_2]^-$ was also carried out when $[(Ph_3P)_2Fe(NO)_2]$ was treated with 1 equiv of $(RS)_2$ and 1 equiv of $[RS]^-$ in CH_3CN at 45 °C. To unambiguously

Scheme 4

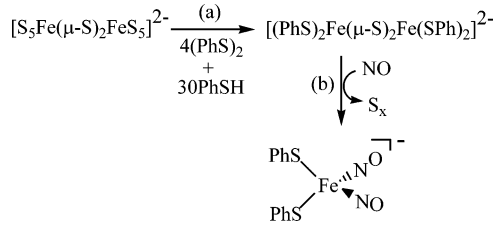

corroborate the formation of $\{Fe(NO)_2\}^9$ $[(RS)_2Fe(NO)_2]^-$ and the proposed transformation mechanism, we treated the CH_3CN solution of $[(Ph_3P)_2Fe(NO)_2]$ and (*S*-2,4,5-Cl_3−$C_6H_2)_2$ (1:1 molar ratio) with 1 equiv of [*S*-*p*-Cl−C_6H_4]$^-$ at 45 °C for 20 h. IR ν_{NO} and UV−vis spectra are consistent with the formation of $[(S\text{-}2,4,5\text{-}Cl_3\text{-}C_6H_2)_2Fe(NO)_2]^-$ (**6**) along with the byproduct (*S*-*p*-Cl−$C_6H_4)_2$ identified by ^1H NMR. This result demonstrates a successful interconversion between $\{Fe(NO)_2\}^9$ DNICs $[(RS)_2Fe(NO)_2]^-$ and $\{Fe(NO)_2\}^{10}$ DNICs $[L_2Fe(NO)_2]$ (L = neutral ligand) under the presence of sodium-biphenyl and thiol/thiolate.

Conversion from $[S_5Fe(\mu\text{-}S)_2FeS_5]^{2-}$ to $\{Fe(NO)_2\}^9$ DNICs. In contrast to inertness of $[S_5Fe(NO)_2]^-$ toward $(PhS)_2$ (or PhSH), conversion of $[S_5Fe(\mu\text{-}S)_2FeS_5]^{2-}$ to the biomimetic ferredoxin $[(PhS)_2Fe(\mu\text{-}S)_2Fe(SPh)_2]^{2-}$ was observed when the CH_3CN solution of $[S_5Fe(\mu\text{-}S)_2FeS_5]^{2-}$, 4 equiv of diphenyl disulfide, and 30 equiv of thiophenol were reacted at 35 °C for 2 h (Scheme 4a). Quantitative conversion of $[S_5Fe(\mu\text{-}S)_2FeS_5]^{2-}$ to $[(PhS)_2Fe(\mu\text{-}S)_2Fe(SPh)_2]^{2-}$ was monitored by UV−vis spectra, the absorption bands at 369, 447 nm disappeared with the formation of one intense absorption band at 477 nm (CH_3CN), and the color changed from yellow brown to purple red. X-ray structural studies also confirmed the formation of complex $[(PhS)_2Fe(\mu\text{-}S)_2Fe(SPh)_2]^{2-}$.[19,20] Upon injecting NO gas into a CH_3CN solution of complex $[(PhS)_2Fe(\mu\text{-}S)_2Fe(SPh)_2]^{2-}$, a rapid reaction ensued over the course of 30 s to give the dark red complex **4** after the reaction solution was precipitated by hexane and extracted by THF (Scheme 4b).[13a] Direct evidence for the conversion of $[S_5Fe(\mu\text{-}S)_2FeS_5]^{2-}$ to the biomimetic ferredoxin $[(RS)_2Fe(\mu\text{-}S)_2Fe(SR)_2]^{2-}$ through the reaction of $[S_5Fe(\mu\text{-}S)_2FeS_5]^{2-}$, thiol, and disulfide and nitrosylation of $[(RS)_2Fe(\mu\text{-}S)_2Fe(SR)_2]^{2-}$ resulting in the degradation of $[(RS)_2Fe(\mu\text{-}S)_2Fe(SR)_2]^{2-}$ to yield $\{Fe(NO)_2\}^9$ DNICs **1**−**4** was provided by UV−vis and IR ν_{NO} spectra.

Structures. Molecular structures of complexes **1**−**3** are given in Figures 3−5, respectively, and the selected bond distances and angles are presented in the figure captions. The N(2)−Fe(1)−N(1) and S(3)−Fe(1)−S(1) bond angles of 116.5(2) and 112.10(6)° in complex **1** (117.17(11) and 112.96(3)° for complex **2**; 117.79(12) and 113.57(3)° for complex **3**) are consistent with the nearly regular tetrahedral coordination environment about Fe. On the basis of Fe−N(O) and N−O bond distances,[14] the average Fe−N and

(19) Hagen, K. S.; Reynolds, J. G.; Holm, R. H. *J. Am. Chem. Soc.* **1981**, *103*, 4054.
(20) (a) Bobrik, M. A.; Hodgson, K. O.; Holm, R. H. *J. Am. Chem. Soc.* **1977**, *16*, 1851. (b) Mayerle, J. J.; Denmark, S. E.; DePamphilis; B. V. Ibers, J. A.; Holm, R. H. *J. Am. Chem. Soc.* **1975**, *97*, 1032−1045.

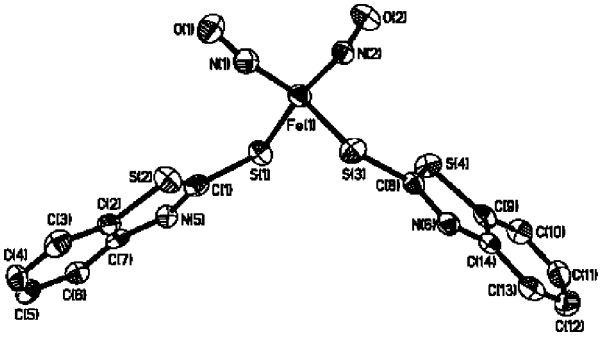

Figure 3. ORTEP drawing and labeling scheme of the $[(NO)_2Fe(2\text{-}S\text{-}C_7H_4NS)_2]^-$ anion. Selected bond distances (Å) and angles (deg): Fe(1)−N(2) 1.680(5); Fe(1)−N(1) 1.687(6); Fe(1)−S(3) 2.2928(18); Fe(1)−S(1) 2.2953(17); N(1)−O(1) 1.174(6); N(2)−O(2) 1.173 (6); N(2)−Fe(1)−N(1) 116.5(2); N(1)−Fe(1)−S(3) 103.47(18); S(1)−Fe(1)−S(3) 112.10(6); O(1)−N(1)−Fe(1) 170.4(5); O(2)−N(2)−Fe(1) 169.4(5).

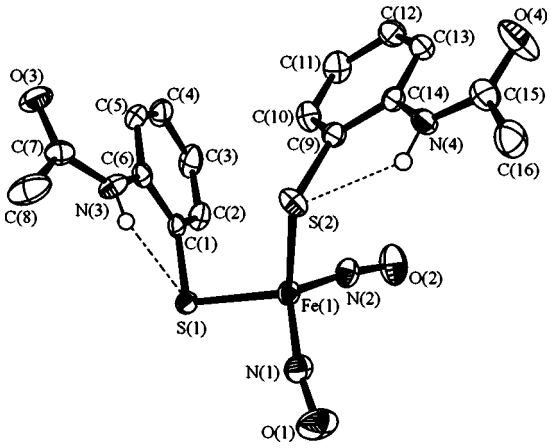

Figure 4. ORTEP drawing and labeling scheme of the $[(NO)_2Fe(SC_6H_4\text{-}o\text{-}NHC(O)CH_3)_2]^-$ anion. Selected bond distances (Å) and angles (deg): Fe(1)−N(2) 1.682(2); Fe(1)−N(1) 1.681(2); Fe(1)−S(2) 2.2805(7); Fe(1)−S(1) 2.3205(7); N(1)-−O(1) 1.174(3); N(2)−O(2) 1.166 (2); N(2)−Fe(1)−N(1) 117.17(11); N(1)−Fe(1)−S(2) 108.32(7); S(1)−Fe(1)−S(2) 112.96(3); O(1)−N(1)−Fe(1) 168.1(2); O(2)−N(2)−Fe(1) 168.5(2).

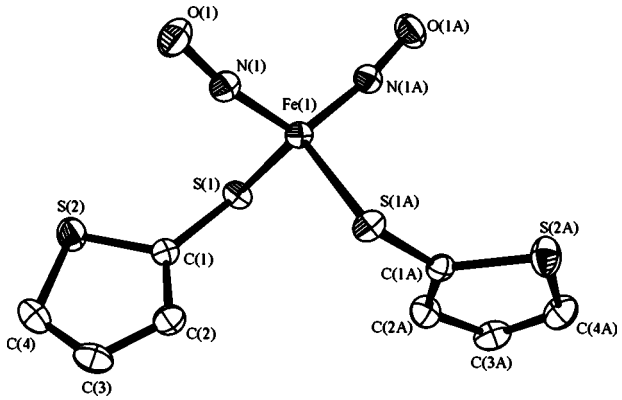

Figure 5. ORTEP drawing and labeling scheme of the $[(NO)_2Fe(2\text{-}S\text{-}C_4H_3S)_2]^-$ anion. Selected bond distances (Å) and angles (deg): Fe(1)−N(1) 1.6832(18); Fe(1)−S(1) 2.2962(6); N(1)−O(1) 1.178(2); O(1)−N(1)−Fe(1) 168.28(17); N(1)−Fe(1)−S(1) 106.75(6); N(1A)−Fe(1)−N(1) 117.79(12); S(1)−Fe(1)−S(1A) 113.57(3).

N−O bond distances of 1.683(6) and 1.173(6) Å for complex **1**, 1.682(2) and 1.170(3) Å for complex **2**, 1.683(2) and 1.178(2) Å for complex **3**, respectively, also support a $\{Fe^+(^\bullet NO)_2\}^9$ electronic structure of $[Fe(NO)_2]$ core of DNICs **1**−**3**.[13a,14] The mean value of the Fe−S bond lengths in

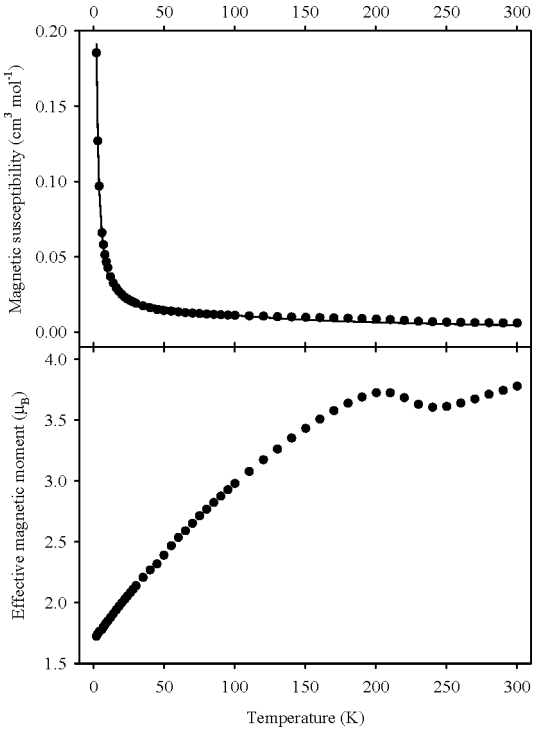

Figure 6. Plots of magnetic susceptibility (top) and effective magnetic moment (bottom) vs temperature for complex **2**. The solid line is the best fit of the data to the appropriate theoretical expression.

complexes **1**−**3** is 2.294(2), 2.301(1), and 2.296(1) Å, respectively, slightly longer than that in complex $[S_5Fe(NO)_2]^-$ (2.288(1) Å).[13a] The X-ray crystal structure of complex **2** shows that the N−H bonds tend to adopt intramolecular [N−H···S] interactions (Figure 4).[17] We also noticed that the S(1)···N(3) distance of 2.954 Å (S(2)···N(3), 2.949 Å) is shorter than the sum (3.270 Å) of S(1)···H(1) and N(3)−H(1) bond distances in complex **2**.

Magnetic Susceptibility Study. Magnetic susceptibility data of a powdered sample of **2** was collected in the temperature range of 2.00−300 K in a 5 kG (0.5 T) applied field. The net molar magnetic susceptibility (χ_M), as shown in Figure 6, increases from 5.946×10^{-3} cm^3 mol^{-1} at 300 K to 0.185 cm^3 mol^{-1} at 2 K. Its corresponding $\chi_M T$ value and effective magnetic moment (μ_{eff}) decrease from 1.785 cm^3 K mol^{-1} (3.779 μ_B) at 300 K to 1.625 cm^3 K mol^{-1} (3.606 μ_B) at 240 K and then increase to a plateau of 1.734 cm^3 K mol^{-1} (3.724 μ_B) at 200 K. After 200 K, the $\chi_M T$ and μ_{eff} values significantly decrease to 0.371 cm^3 K mol^{-1} (1.722 μ_B) at 2 K. From a magnetochemical point of view, the $\{Fe^+(^\bullet NO)_2\}^9$ unit is considered as a tri-spin system. The spin-only ($g = 2.00$) $\chi_M T$ and μ_{eff} values for three magnetically independent centers ($S_1 = {}^3/_2$, $S_2 = S_3 = {}^1/_2$) are 2.625 cm^3 K mol^{-1} and 4.583 μ_B, respectively. The spin-only values for a $S = {}^5/_2$ system are 4.375 cm^3 K mol^{-1} and 5.916 μ_B, respectively. Relatively large $\chi_M T$ and μ_{eff} values of complex **2** at 300 K are not consistent with the long-believed understanding, 0.375 cm^3 K mol^{-1} (1.732 μ_B), for ground state $S_T = {}^1/_2$ in the $\{Fe^+(^\bullet NO)_2\}^9$ core due to the strong antiferromagnetic interactions between the Fe^+ (d^7, $S = {}^3/_2$) center and two $^\bullet NO$ ($S = {}^1/_2$) radicals.

The theoretical equations for data-fitting are derived from the Heisenberg Hamiltonian ($\hat{H} = -2J\,\hat{S}_1\,\hat{S}_2$) and the Van-Vleck equation for a single-*J*-value system in which *J* is the exchange parameter between the Fe^+ ion and the $^\bullet NO$ radical under approximation of an ideal C_{2v} symmetry.[21] Representation of the electronic state based on the Enemark-Feltham model as $\{Fe(NO)_2\}^9$ for complex **2** is due to the variable nature of NO coordinated to a transition metal as $M-NO^+$, $M-NO^\bullet$, and $M-NO^-$.[15] If only the lowest energy electronic state is considered, both $\{Fe^+(^\bullet NO)_2\}^9$ and $\{Fe^-(^+NO)_2\}^9$ in DNICs **2** are possible. Both states are paramagnetic. The former has its S_T either of $^5/_2$ or of $^1/_2$. The latter consists of a spin-only value of $^1/_2$. The experimental magnetic susceptibility may be contributed from both electronic states if mixed electronic states are present in **2**, as shown below. Due to the undetermined exclusive electronic state of complex **2**, fitting of the magnetic data is based on the assumption of the presence of both electronic states.

$$\chi_M^{exp} = (1\text{-}p)\,\chi_M(\{Fe^+(^\bullet NO)_2\}^9) + p\,\chi_M(\{Fe^-(^+NO)_2\}^9)$$

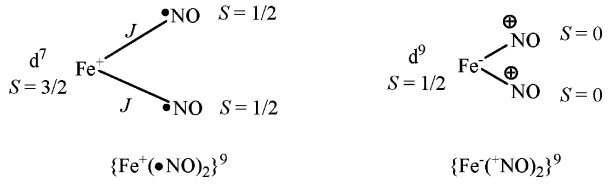

$\{Fe^+(\bullet NO)_2\}^9$ $\{Fe^-(^+NO)_2\}^9$

A least-squares fit ($R^2 = 0.996$) to the χ_M vs temperature (2−300 K) curve, shown as a solid line in Figure 6, gave $2J = -27(2)$ cm^{-1}, $g = 2.02(1)$, $p = 0.545(38)$, with TIP (temperature-independent paramagnetism) held constant at 200×10^{-6} cm^3 mol^{-1}. The result from the fit indicates that the Fe^+ center is antiferromagnetically coupled to the $^\bullet NO$ radicals and the electronic state $\{Fe^+(^\bullet NO)_2\}^9$ is not dominant in **2**. On the other hand, albeit complex **2** shares the same $\{Fe(NO)_2\}^9$ motif as $[S_5Fe(NO)_2]^-$ does, relatively large $\chi_M T$ value of **2**, which significantly differs from that of $[S_5Fe(NO)_2]^-$ (0.527 cm^3 K mol^{-1}), insinuates different ratios of $\{Fe^+(^\bullet NO)_2\}^9$ and $\{Fe^-(^+NO)_2\}^9$ in both complexes.[13a] Complex $[S_5Fe(NO)_2]^-$ possesses a higher percentage of $\{Fe^-(^+NO)_2\}^9$ than **2** does. In other words, complex **2** has a greater ability for NO liberation, which is consistent with the results in the NO-trapping experiments. In the presence of $[Fe(S,S\text{-}C_6H_4)_2]_2^{2-}$, its reaction rate to remove NO from **2** is approximately 10-fold faster than that from $[S_5Fe(NO)_2]^-$, as shown in Figure 1. Obviously, such drastic influence comes from the different electron-donating thiolate ligands coordinated to the $\{Fe(NO)_2\}^9$ motif.

When part of the $\chi_M - T$ curve was taken for data-fitting, satisfactory results were also obtained from the least-squares fits for three selected varied temperature ranges: $R^2 = 0.999$, $2J = -6(1)$ cm^{-1}, $g = 1.99(1)$, $p = 0.928(10)$ for $T = 2-20$ K; $R^2 = 0.998$, $2J = -16(1)$ cm^{-1}, $g = 2.01(1)$, $p = 0.749(27)$ for $T = 2-100$ K; $R^2 = 0.996$, $2J = -22(2)$ cm^{-1}, $g = 2.02(1)$, $p = 0.634(4)$ for $T = 2-180$ K, respectively. Variation of the *p* value from the magnetic susceptibility fit in different temperature ranges indicates that the resonance hybrid of $\{Fe^+(^\bullet NO)_2\}^9$ and $\{Fe^-(^+NO)_2\}^9$ in **2** is dynamic by temperature.[22] It implicates that both temperature and the ability of the thiolate ligands as an electron donor to the $\{Fe(NO)_2\}^9$ motif correlate with its electronic states and play the critical role in regulating NO release of DNICs. Detailed magnetochemistry of related DNICs are currently under further investigation.

(21) Kahn, O. *Molecular Magnetism*; VCH: New York, 1993.

Conclusion and Comments

Studies on the dinitrosyl iron complexes **1**−**4** have led to the following results.

1. $\{Fe(NO)_2\}^9$ DNICs $[(RS)_2Fe(NO)_2]^-$ may serve as NO-donor species. The coordinated thiolate ligands of $\{Fe(NO)_2\}^9$ DNICs $[(RS)_2Fe(NO)_2]^-$ can therefore finely regulate NO-release activity and stability (isolation) of $\{Fe(NO)_2\}^9$ DNICs $[(RS)_2Fe(NO)_2]^-$. DNICs containing the less electron-donating thiolate ligands coordinated to $\{Fe(NO)_2\}^9$ motif act as the better NO-donor DNICs in the presence of NO-trapping agents $[Fe(S,S\text{-}C_6H_4)_2]_2^{2-}/[(C_4H_8O)Fe(S,S\text{-}C_6H_4)_2]^-$.

2. The stronger electron-donating thiolates $[R'S]^-$, compared to the coordinated thiolate ligands of the dinitrosyl iron complexes $[(RS)_2Fe(NO)_2]^-$, may promote thiolate-ligand exchange to produce the stable LMW-DNICs $[(R'S)_2Fe(NO)_2]^-$.

3. The stronger electron-donating coordinated thiolates of DNICs $[(R'S)_2Fe(NO)_2]^-$, compared to the thiolates $[RS]^-$, may trigger S−S bond activation of the disulfide species ($[RS]_2$) to yield the stable DNICs $[(RS)_2Fe(NO)_2]^-$.

4. The range of IR ν_{NO} stretching frequencies (ranging from (1766, 1716) to (1737, 1693) cm^{-1} (THF)) of complexes **1**−**4** observed in this study represents the entire window of possible electronic configurations for such stable and isolable $\{Fe(NO)_2\}^9$ $[(RS)_2Fe(NO)_2]^-$.

5. Reductant sodium-biphenyl may trigger the conversion of the $\{Fe(NO)_2\}^9$ DNICs $[(SR)_2Fe(NO)_2]^-$ to $\{Fe(NO)_2\}^{10}$ DNICs $[(Ph_3P)_2Fe(NO)_2]$ in the presence of PPh_3.

6. Two routes lead to the formation of $\{Fe(NO)_2\}^9$ LMW-DNICs: (i) direct nitrosylation of [Fe−S] clusters (e.g., $[S_5Fe(\mu\text{-}S)_2FeS_5]^{2-}$ and $[(RS)_2Fe(\mu\text{-}S)_2Fe(SR)_2]^{2-}$),[13a] (ii) transformation of $\{Fe(NO)_2\}^{10}$ $[L_2Fe(NO)_2]$ (L = neutral N-/P-containing ligands) to $\{Fe(NO)_2\}^9$ $[(RS)_2Fe(NO)_2]^-$ promoted by 2 equiv of thiols and thiolate ($2RSH + [RS]^-$ or $(RS)_2 + [RS]^-$).

7. The result from the magnetic susceptibility fit indicates that the Fe^+ center is antiferromagnetically coupled to the $^\bullet NO$ radicals ($2J = -27(2)$ cm^{-1}) and the electronic state $\{Fe^+(^\bullet NO)_2\}^9$ is not dominant in **2**. Variation of the *p* value from the magnetic susceptibility fit ($\chi_M^{exp} = (1-p)\,\chi_M(\{Fe^+(^\bullet NO)_2\}^9) + p\,\chi_M(\{Fe^-(^+NO)_2\}^9)$) in different temperature ranges indicates that the resonance hybrid of $\{Fe^+(^\bullet NO)_2\}^9$ and $\{Fe^-(^+NO)_2\}^9$ in **2** is dynamic by temperature. Furthermore, the electronic structure of $\{Fe(NO)_2\}$ core of $\{Fe(NO)_2\}^9$ DNICs $[(RS)_2Fe(NO)_2]^-$ is best described

(22) (a) Hsieh, C.-H.; Hsu, I.-J.; Lee, C.-M.; Ke, S.-C.; Wang, T.-Y.; Lee, G.-H.; Wang, Y.; Chen, J.-M.; Lee, J.-F.; Liaw, W.-F. *Inorg. Chem.* **2003**, *42*, 3925. (b) Herebian, D.; Bothe, E.; Bill, E.; Weyhermuller, T.; Wieghardt, K. *J. Am. Chem. Soc.* **2001**, *123*, 10012.

Scheme 5

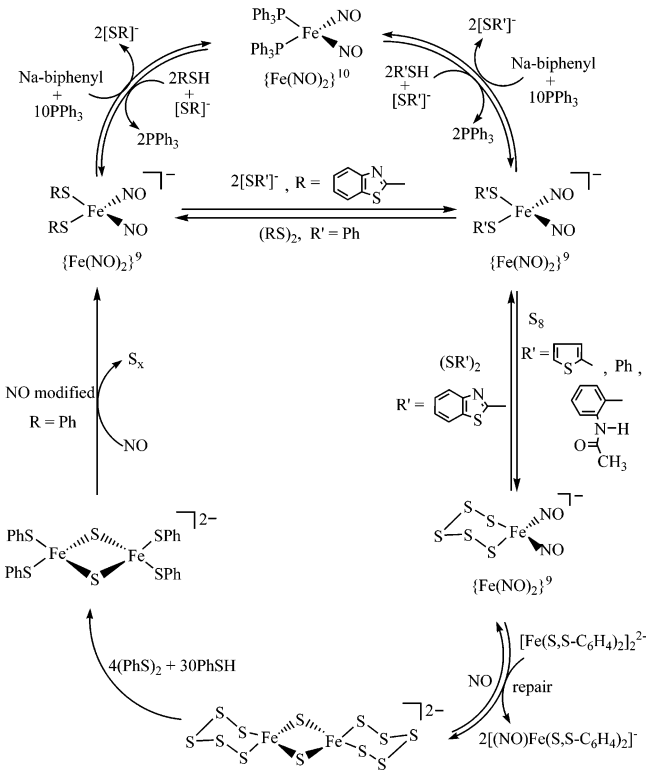

as a resonance hybrid of $\{Fe^+(^\bullet NO)_2\}^9$ and $\{Fe^-(^+NO)_2\}^9$ controlled by the coordinated thiolate ligands.[22]

On the basis of this investigation and related observation,[13a,13c] it is presumed that binding of the polarizable anionic thiolate-donor ligands (the electron-donating strength, generally, ranges from $[SPh]^-$ to $[-SC_7H_4SN]^-$) to $[Fe(NO)_2]$ motif places $\{Fe(NO)_2\}^9$ $[(RS)_2Fe(NO)_2]^-$ in an optimum electronic condition to stabilize $[(RS)_2Fe(NO)_2]^-$. The $\{Fe(NO)_2\}^9$ DNICs $[(RS)_2Fe(NO)_2]^-$ may act as NO-donor species, and presumably, only the reduced form $\{Fe(NO)_2\}^{10}$ $[(RS)(L)Fe(NO)_2]^-$ (RS = thiolates; L = neutral ligand) and the oxidized form $[(RS)_2Fe(NO)_2]$ containing a $\{Fe(NO)_2\}^8$ electronic core may undergo ligand exchange and reduction to form neutral $\{Fe(NO)_2\}^{10}$ and anionic $\{Fe(NO)_2\}^9$ DNICs, respectively.

As shown in Scheme 5, a biomimetic reaction cycle derived from this study may decipher and predict the biological cycle of interconversion of $\{Fe(NO)_2\}^9$ DNICs, $\{Fe(NO)_2\}^{10}$ DNICs, and the [Fe−S] clusters in proteins. LMW-DNICs, responsible for the formation of *S*-nitrosothiol, has been proposed to be produced by reaction of the low-molecular-weight thiol and protein-bound DNIC via thiol-ligand exchange mechanism.[4−7] The mechanism for *S*-nitrosation of proteins by LMW-DNICs and the detailed magnetochemistry of related DNICs will be explored in the future study.

Experimental Section

Manipulations, reactions, and transfers were conducted under nitrogen according to Schlenk techniques or in a glovebox (argon gas). Solvents were distilled under nitrogen from appropriate drying agents (diethyl ether from CaH_2; acetonitrile from $CaH_2-P_2O_5$; methylene chloride from CaH_2; hexane and tetrahydrofuran (THF) from sodium benzophenone) and stored in dried, N_2-filled flasks over 4 Å molecular sieves. Nitrogen was purged through these solvents before use. Solvent was transferred to the reaction vessel via a stainless cannula under positive pressure of N_2. The reagents sulfur powder (Showa), di(2-thienyl)disulfide, thiophenol, 2,3,4-trichlorophenyl disulfide, *p*-chlorophenyl disulfide, *p*-chlorothiophenol, diphenyl disulfide, iron pentacarbonyl, sodium nitrite (Aldrich), bis(2-benzothiozolyl) disulfide, and bis(triphenylphosphoranylidene)ammonium chloride ([PPN][Cl]) (Fluka) were used as received. Compounds $[PPN][(NO)_2FeS_5]$,[13a] $[Fe(S,S\text{-}C_6H_4)_2]_2^{2-}$,[13b] $[(C_4H_8O)Fe(S,S\text{-}C_6H_4)_2]^-$,[13b] $[PPN][HFe(CO)_4]$,[23] $(Ph_3P)_2Fe(NO)_2$,[24] and 2-(acetylamino)phenyl disulfide were synthesized by published procedures.[17c,19] Infrared spectra of the ν(NO) and ν(NH) stretching frequencies were recorded on a Perkin-Elmer model spectrum one B spectrophotometer with sealed solution cells (0.1 mm, KBr windows) or KBr solid. UV−vis spectra were recorded on a GBC Cintra 10e and Jasco V-570. ^{1}H spectra were obtained on a Varian Unity-500 spectrometer. Electrochemical measurements were performed with CHI model 421 potentionstat (CH Instrument) instrumentation. Cyclic voltammograms were obtained from 1.25 mM analyte concentration in MeCN using 0.05 M $[n\text{-}Bu_4N][PF_6]$ as a supporting electrolyte. Potentials referenced to a Ag/AgCl reference electrode were measured at 298 K by use of a glassy carbon working electrode and a Pt counter electrode at a scan rate of 1 V s^{-1}. Under the conditions employed, the potential of the ferrocenium/ferrocene couple was 0.39 V. Analyses of carbon, hydrogen, and nitrogen were obtained with a CHN analyzer (Heraeus).

Preparation of [cation][(2-*S*-$C_7H_4NS)_2Fe(NO)_2$] (1) (cation = PPN, Na-18-crown-6-ether). Compounds $[PPN][S_5Fe(NO)_2]$ (0.163 g, 0.2 mmol) and bis(2-benzothiozolyl) disulfide (0.0665 g, 0.2 mmol) were dissolved in THF (10 mL) and stirred overnight under nitrogen at ambient temperature. The reaction was monitored with FTIR. IR spectra (ν_{NO}: 1716 s, 1766 s cm^{-1} (THF)) were assigned to the formation of $[PPN][(2\text{-}S\text{-}C_7H_4NS)_2Fe(NO)_2]$. The solution was then concentrated and hexane-diethyl ether (10:10 mL volume ratio) was added to precipitate the dark-red solid $[PPN][(2\text{-}S\text{-}C_7H_4NS)_2Fe(NO)_2]$ (**1**) (0.190 g, 93%). Alternatively, $[PPN][HFe(CO)_4]$ (0.353 g, 5 mmol) and bis(2-benzothiazolyl) disulfide (0.333 g, 10 mmol) were loaded into a 20-mL Schlenk tube and dissolved in THF (10 mL). After being stirred for 20 min at ambient temperature, the mixture solution was transferred to another Schlenk flask containing $[PPN][NO_2]$ (0.584 g, 10 mmol) by a cannula under positive N_2 pressure. The reaction mixture was stirred for 5 h at 45 °C, and the mixture solution was filtered through Celite. The filtrate was collected, and hexane was added to precipitate the dark red solid complex **1** (yield 80%). Diffusion of diethyl ether−hexane into the THF solution of complex **1** at −15 °C led to dark red crystals suitable for single-crystal X-ray diffraction. IR (ν_{NO}): 1716, 1766 cm^{-1} (THF); 1721, 1773 cm^{-1} (CH_3CN). Absorption spectrum (THF) [λ_{max}, nm (ϵ, M^{-1} cm^{-1})]: 465 (3501), 799 (712). Anal. Calcd for $C_{26}H_{32}N_4O_8S_4FeNa$: C, 42.41; H, 4.35; N, 7.61. Found: C, 42.13; H, 4.22; N, 7.36.

Preparation of [PPN][$(SR)_2Fe(NO)_2$] (R = C_6H_4-*o*-NHC(O)-CH_3 (2); C_4H_3S (3); C_6H_5 (4)). Compounds $[PPN][(2\text{-}S\text{-}C_7H_4NS)_2Fe(NO)_2]$ (0.098 g, 1 mmol) and [PPN][SR] (R = C_6H_4-*o*-$NHCOCH_3$ (0.15 g, 2 mmol); C_4H_3S (0.13 g, 2 mmol); C_6H_5 (0.13 g, 2 mmol)) were dissolved in acetonitrile (10 mL) and stirred for

(23) Liaw, W.-F.; Lee, J.-H.; Gau, H.-B.; Chen, C.-H.; Lee, G.-H. *Inorg. Chim. Acta* **2001**, *322*, 99−105.
(24) McBride, D. W.; Stafford, S. L.; Stone, F. G. A. *Inorg. Chem.* **1962**, *1*, 386−388.

5 min at ambient temperature. Solvent was then removed under vacuum. The crude solid was redissolved in THF (10 mL) and then filtered through Celite to remove the insoluble [PPN][2-*S*-C_7H_4-NS]. Addition of hexane (15 mL) to the filtrate led to precipitation of dark solid [PPN][$(SR)_2Fe(NO)_2$] (R = C_6H_4-*o*-NHC(O)CH_3 (**2**) (80%); C_4H_3S (**3**) (67%); C_6H_5 (**4**) (93%)). Diffusion of diethyl ether−hexane into the THF solution of complexes **2**, **3**, and **4**, respectively, led to dark crystals suitable for single-crystal X-ray diffraction. Complex **2**: IR: 1752, 1705 (ν_{NO}), 1690 (ν_{CO}) cm^{-1} (THF); 1757, 1707 (ν_{NO}), 1682 (ν_{CO}), 3303 (ν_{NH}) cm^{-1} (CH_2Cl_2); 1754, 1709 (ν_{NO}), 1688 (ν_{CO}), 3303 (br) (ν_{NH}) cm^{-1} (KBr). Absorption spectrum (THF) [λ_{max}, nm (ϵ, M^{-1} cm^{-1})]: 479 (2984), 774 (453). Anal. Calcd for $C_{52}H_{46}N_5O_4P_2S_2Fe$: C, 63.23; H, 4.66; N, 7.09. Found: C, 63.29; H, 4.60; N, 7.17. Complex **3**: IR ν_{NO} (THF): 1743, 1698 cm^{-1}. Absorption spectrum (THF) [λ_{max}, nm (ϵ, M^{-1} cm^{-1})]: 514 (2834), 798 (901). Anal. Calcd for $C_{44}H_{36}N_3O_2P_2S_4Fe$: C, 59.66; H, 4.06; N, 4.74. Found: C, 60.16; H, 4.32; N, 4.67. Complex **4**: IR ν_{NO} (THF): 1737, 1693 cm^{-1}.[16b]

Reaction of [PPN][$(SC_6H_5)_2Fe(NO)_2$] and Disulfides $(RS)_2$ (R = 2-C_7H_4NS, C_6H_4-*o*-NHC(O)CH_3, C_4H_3S). A THF solution of [PPN][$(PhS)_2Fe(NO)_2$] (0.086 g, 1 mmol) was transferred to a 50-mL Schlenk flask loaded with disulfide species $(RS)_2$ (R = C_7H_4-NS (0.035 g, 1 mmol), C_6H_4-*o*-NHC(O)CH_3 (0.035 g, 1 mmol); C_4H_3S (0.024 g, 1 mmol)) by a cannula under positive N_2 pressure at room temperature. The reaction mixture was stirred for 1 h at room temperature, and hexane (15 mL) was added to precipitate the dark solid [PPN][$(RS)_2Fe(NO)_2$] (R = C_7H_4NS (**1**) (yield 93%); C_6H_4-*o*-NHC(O)CH_3 (**2**) (95%); C_4H_3S (**3**) (90%)) characterized by IR, UV−vis, and single-crystal X-ray diffraction.

Characterization of ν_{CO} and ν_{NO} Stretching Frequencies of Complex 2. Compounds [PPN][$HFe(CO)_4$] (0.142 g, 2 mmol) and bis(2-benzothiazolyl) disulfide (0.133 g, 4 mmol) were loaded into a 20-mL Schlenk tube and dissolved in THF (10 mL). After being stirred for 20 min at ambient temperature, the red-yellow solution was transferred to another Schlenk flask loaded with [PPN][$^{15}NO_2$] (0.234 g, 4 mmol) by a cannula under positive N_2 pressure. The reaction mixture was stirred for 5 h at 45 °C. The mixture solution was filtered through Celite, and hexane was added to precipitate the dark red solid [PPN][$(2\text{-}S\text{-}C_7H_4NS)_2Fe(^{15}NO)_2$]. Acetonitrile solution of [PPN][$(2\text{-}S\text{-}C_7H_4NS)_2Fe(^{15}NO)_2$] was transferred to a 50-mL flask loaded with [PPN][SC_6H_4-*o*-NHC(O)CH_3] (0.282 g, 4 mmol) and then stirred for 5 min at ambient temperature. Solvent was removed under vacuum. The crude solid was then redissolved in THF (10 mL) and filtered through Celite to remove the insoluble [PPN][2-*S*-C_7H_4NS]. Addition of hexane (15 mL) to the filtrate led to precipitation of dark red-brown solid [PPN][$(SC_6H_4$-*o*-NHC(O)$CH_3)_2Fe(^{15}NO)_2$] (66%) characterized by IR and UV−vis spectrum (IR (THF): 1718 s, 1673 vs (ν_{NO}), 1690 vs (ν_{CO}) cm^{-1}. Absorption spectrum (THF) [λ_{max}, nm (ϵ, M^{-1} cm^{-1})]: 479 (2984), 774 (453)).

Reaction of [PPN][$(RS)_2Fe(NO)_2$] and S_8 (R = C_6H_4-*o*-NHCOCH_3 (2); C_4H_3S (3); C_6H_5 (4)). A THF solution of [PPN][$(RS)_2Fe(NO)_2$] (R = C_6H_4-*o*-NHC(O)CH_3 (**2**) (0.0987 g, 1 mmol); C_4H_3S (**3**) (0.0885 g, 1 mmol); C_6H_5 (**4**) (0.0873 g, 1 mmol)), respectively, was transferred to a 50-mL Schlenk flask loaded with sulfur powder S_8 (0.026 g, 1 mmol) by a cannula under positive N_2 pressure. The reaction mixture was stirred for 2 h at ambient temperature, and then hexane (15 mL) was added to precipitate the dark green solid [PPN][$S_5Fe(NO)_2$] (yield 80%) characterized by IR, UV−vis spectrum, and single-crystal X-ray diffraction.

Transformation of $Fe(NO)_2(PPh_3)_2$ to [PPN][$(RS)_2Fe(NO)_2$] (R = C_6H_5 (4), *p*-Cl-C_6H_4 (5), 2,4,5-Cl_3-C_6H_2 (6)). Compounds $Fe(NO)_2(PPh_3)_2$ (0.1280 g, 0.2 mmol), $(SR)_2$ (or 2 equiv of thiol RSH) (R = C_6H_5 (0.0436 g, 0.2 mmol), *p*-Cl-C_6H_4 (0.0574 g, 0.2 mmol), 2,4,5-Cl_3-C_6H_2 (0.0850 g, 0.2 mmol)), and [PPN][SR] (R = C_6H_5 (0.0648 g, 0.1 mmol), *p*-Cl-C_6H_4 (0.0682 g, 0.1 mmol), 2,4,5-Cl_3-C_6H_2 (0.1 mmol)) were dissolved in CH_3CN (8 mL) and stirred under nitrogen at 45 °C for 20 h. After CH_3CN was removed under vacuum, the crude residues were redissolved in THF (5 mL). Diethyl ether (7 mL) was added and then the resulting mixture was filtered through Celite. The filtrate was concentrated, and hexane (10 mL) was added to precipitate the dark red solid [PPN][$(RS)_2Fe(NO)_2$] (R = C_6H_5 (**4**) (45%), *p*-Cl-C_6H_4 (**5**) (50%), 2,4,5-Cl_3-C_6H_2 (**6**) (44%)) characterized by IR and UV−vis spectrum. Complex **5**: IR ν_{NO}: 1742, 1698 (THF); 1748, 1702 cm^{-1} (CH_3CN). Absorption spectrum (THF) [λ_{max}, nm (ϵ, M^{-1} cm^{-1})]: 486 (1812), 791 (405). Complex **6**: IR ν_{NO}: 1755, 1708 (THF); 1760, 1713 cm^{-1} (CH_3CN). Absorption spectrum (THF) [λ_{max}, nm (ϵ, M^{-1} cm^{-1})]: 474 (2441), 800 (494).

Reaction of Complexes 1, PPh_3, and Sodium-biphenyl. To a THF solution (5 mL) of complex **1** (98.7 mg, 0.1 mmol) and 10 equiv of triphenylphosphine (0.263 g, 1 mmol) was added a THF solution of sodium-biphenyl (0.8 mL from 30 mL of stock solution prepared by mixing 4.62 g of biphenyl and 0.69 g of sodium) by a cannula under positive N_2 pressure at −40 °C. The reaction was monitored by FTIR immediately. The ν_{NO} spectrum shows two strong absorption bands at 1682, 1639 cm^{-1} temporarily assigned as the formation of the unstable, reduced $\{Fe(NO)_2\}^{10}$ [(2-*S*-C_7H_4-NS)$(Ph_3P)Fe(NO)_2]^-$ intermediate. The reaction mixture was stirred at ambient temperature overnight and then the solvent was removed under vacuum. Neutral $(PPh_3)_2Fe(NO)_2$ was extracted with diethyl ether and hexane was added to precipitate the known neutral $(PPh_3)_2$-$Fe(NO)_2$ characterized by IR and UV−vis spectra.[24] $(PPh_3)_2$-$Fe(NO)_2$ was recrystallized in diethyl ether−hexane (yield 17 mg, 26%).

Reaction of $[PPN]_2[S_5Fe(\mu\text{-}S)_2FeS_5]$, Thiophenol, and Diphenyl Disulfide. Compounds $[PPN]_2[S_5Fe(\mu\text{-}S)_2FeS_5]$ (0.078 g, 0.5 mmol) (absorption spectrum (CH_3CN) [λ_{max}, nm (ϵ, M^{-1} cm^{-1})]: 369 (9102), 447 (13159))[13a] and diphenyl disulfide (0.043 g, 2 mmol) dissolved in acetonitrile (15 mL) were transferred to a 50-mL flask loaded with thiophenol (0.15 mL, 15 mmol) under positive N_2 pressure. The reaction mixture was stirred at 35 °C for 2 h, and then diethyl ether (15 mL) was added to precipitate dark purple-red solid $[PPN]_2[(C_6H_5S)_2Fe(\mu\text{-}S)_2Fe(SC_6H_5)_2]$ (yield 0.022 g, 25%) characterized by UV−vis spectrum and single-crystal X-ray diffraction. Diffusion of diethyl ether into the acetonitrile solution of the known $[PPN]_2[(C_6H_5S)_2Fe(\mu\text{-}S)_2Fe(SC_6H_5)_2]$ at −15 °C led to dark purple-red crystals suitable for single-crystal X-ray diffraction. Absorption spectrum (CH_3CN) [λ_{max}, nm (ϵ, M^{-1} cm^{-1})]: 477 (14508).[20b]

Injection of NO(g) into CH_3CN Solution of $[(C_6H_5S)_2Fe(\mu\text{-}S)_2Fe(SC_6H_5)_2]^{2-}$. A CH_3CN solution (10 mL) of $[(C_6H_5S)_2Fe(\mu\text{-}S)_2Fe(SC_6H_5)_2]^{2-}$ (0.042 g, 0.25 mmol) was purged with NO gas for 30 s at ambient temperature. After the reaction solution was stirred for 20 min, the dark red solution was filtered and the dark red product was precipitated by addition of diethyl ether−hexane. The IR spectrum (ν_{NO} (THF): 1737, 1693 cm^{-1}) was assigned to the formation of [PPN][$(PhS)_2Fe(NO)_2$] (**4**) (65%).[16a,b] Recrystallization from saturated THF solution with hexane diffusion gave dark red crystals of complex **5**, identified by single-crystal X-ray diffraction.

Reactions of DNICs 1−4, $[S_5Fe(NO)_2]^-$, and $[PPN]_2[Fe(S,SC_6H_4)_2]_2$, Respectively. For comparisons of NO-releasing activity of DNICs **1**, **2**, **3**, **4**, and $[S_5Fe(NO)_2]^-$, the reaction time courses of NO release trapped by 1 equiv of $[PPN]_2[Fe(S,SC_6H_4)_2]_2$ for **1**−**4** and $[S_5Fe(NO)_2]^-$ in DMSO at 18 °C were studied by

monitoring the formation of product $[PPN][(NO)Fe(S,SC_6H_4)_2]$ with intense absorption at 1298 nm. The concentration of complexes **1**, **2**, **3**, **4**, and $[S_5Fe(NO)_2]^-$ is 1.1×10^{-3} M, respectively. A vial (10 mL) loaded with DMSO (4 mL) of $[PPN]_2[Fe(S,SC_6H_4)_2]_2$ (7.8 mg, 0.0044 mmol) was sealed with a septum and tied with copper wire/Parafilm. Super sonicator was applied for 3 min to dissolve $[PPN]_2[Fe(S,S\text{-}C_6H_4)_2]_2$ in DMSO. The same equivalents of DNICs **1** (4.3 mg) (**2** (4.3 mg), **3** (3.9 mg), **4** (3.9 mg), and $[S_5Fe(NO)_2]^-$ (3.6 mg)) were ground and loaded into a septum-sealed UV cell wrapped with aluminum foil in the glovebox in the dark. DMSO solution of $[PPN]_2[Fe(S,S\text{-}C_6H_4)_2]_2$ was then added to the UV cell loaded with DNICs **1**−**4** and $[S_5Fe(NO)_2]^-$ via syringe, respectively. The mixture solution was shaken quickly and then monitored immediately by UV−vis. The collected data were analyzed by Excel/Origin program. It has been known that $[PPN][(NO)Fe(S,S\text{-}C_6H_4)_2]$ was reduced to yield $[PPN]_2[(NO)Fe(S,S\text{-}C_6H_4)_2]$ in the presence of $[RS]^-$.[14] To prevent the reduction of $[PPN][(NO)Fe(S,S\text{-}C_6H_4)_2]$ caused by thiolates derived from decomposition of the intermediate $[(RS)_2Fe]$ resulting from NO release of DNICs **1**−**4**, data of the reaction time courses of NO release in the presence of NO-trapping reagent $[PPN]_2[Fe(S,SC_6H_4)_2]_2$ were collected in the interval of the first 100 s. Since $[(NO)Fe(S,S\text{-}C_6H_4)_2]^-$ was reduced to yield $[(NO)Fe(S,S\text{-}C_6H_4)_2]^{2-}$ in the presence of $[RS]^-$ derived from decomposition of the intermediate $[(RS)_2Fe]$, the k_{obs} data of the reactions of complexes **1**−**4** and $[(NO)Fe(S,S\text{-}C_6H_4)_2]^{2-}$ respectively, were unable to be collected. The k_{obs} of the reaction of $[S_5Fe(NO)_2]^-$ and $[PPN]_2[Fe(S,S\text{-}C_6H_4)_2]_2$ was conducted under pseudo-first-order condition in the ratio 1:20 at 18 °C.

EPR Measurements. EPR measurements were performed at X-band using a Bruker EMX spectrometer equipped with a Bruker TE102 cavity. The microwave frequency was measured with a Hewlett-Packard 5246L electronic counter. X-band EPR spectra of complexes **2** and **3** in THF were obtained with a microwave power of 20.02 mW, frequency at 9.605 GHz, and modulation amplitude of 0.2 G at 100 kHz.

Magnetic Measurements. The magnetic data were recorded on a SQUID magnetometer (MPMS5 Quantum Design Company) under a 0.5 T external magnetic field in the temperature range of 2−300 K. The magnetic susceptibility data were corrected with temperature-independent paramagnetism (TIP, 2×10^{-4} cm^3 mol^{-1}) and ligands' diamagnetism by the tabulated Pascal's constants. The equation for one J spin-coupled system is derived from the Hamiltonian and Van-Vleck's equation.[21] The magnetic coupling constant J of **2** is obtained from the least-squares fit of the magnetic susceptibility data.

Crystallography. Crystallographic data and structure refinements parameters of complexes **1**, **2**, and **3** are summarized in the Supporting Information. Each crystal was mounted on a glass fiber and quickly coated in epoxy resin. Unit-cell parameters were obtained by least-squares refinement. Diffraction measurements for complexes **1**, **2**, and **3** were carried out on a SMART Apex CCD diffractometer with graphite-monochromated Mo Kα radiation (λ = 0.7107 Å). Least-squares refinement of the positional and anisotropic thermal parameters of all non-hydrogen atoms and fixed hydrogen atoms was based on F^2. A SADABS[25] absorption correction was made. The SHELXTL[26] structure refinement program was employed.

Acknowledgment. We gratefully acknowledge financial support from the National Science Council (Taiwan).

Supporting Information Available: X-ray crystallographic file in CIF format for the structure determinations of $[PPN][(NO)_2Fe(2\text{-}S\text{-}C_7H_4NS)_2]$, $[PPN][(NO)_2Fe(SC_6H_4\text{-}o\text{-}NHC(O)CH_3)_2]$, $[PPN][(NO)_2Fe(2\text{-}S\text{-}C_4H_3S)_2]$, and $[PPN]_2[(PhS)_2Fe(\mu\text{-}S)_2Fe(SPh)_2]$. This material is available free of charge via the Internet at http://pubs.acs.org.

IC0505044

(25) Sheldrick, G. M. *SADABS, Siemens Area Detector Absorption Correction Program*; University of Göttingen: Göttingen, Germany, 1996.
(26) Sheldrick, G. M. *SHELXTL, Program for Crystal Structure Determination;* Siemens Analytical X-ray Instruments Inc.: Madison, WI, 1994.